CONF-840708--1

DISCLAIMER

NONRELATIVISTIC THEORY OF HEAVY-ION COLLISIONS

G. Bertsch
Department of Physics
University of Tennessee
Knoxville, TN 37996

and

Physics Division
Oak Ridge National Laboratory
Oak Ridge, TN 37831

CONF-840708--1

DE85 007538

Invited paper presented at

School in Heavy-Ion Physics
Erice, Sicily
July 17-23, 1984

NONRELATIVISTIC THEORY OF HEAVY-ION COLLISIONS

C. Bertsch

Department of Physics
University of Tennessee
Knoxville, TN 37996

and

Oak Ridge National Laboratory*
Oak Ridge, TN 37831

INTRODUCTION

A wide range of phenomena is observed in heavy-ion collisions, calling for a comprehensive theory based on fundamental principles of many-particle quantum mechanics. At low energies, the nuclear dynamics is controlled by the mean field, as we know from spectroscopic nuclear physics. We therefore expect the comprehensive theory of collisions to contain mean-field theory at low energies. The mean-field theory will be the subject of the first lectures in this chapter. This theory can be studied quantum mechanically, in which form it is called TDHF (time-dependent Hartree-Fock), or classically, where the equation is called the Vlasov equation.

At high energies the mean field becomes insignificant in comparison with the effects of nucleon-nucleon collisions. A proper theory needs to include collision effects, as is done in the classical theory of gases with the Boltzmann equation. The lectures will go on from mean-field theory to the derivation of theories incorporating collisions. Again, there are both quantum and classical extensions of mean-field theory. The classical equation turns out to

*Operated by Martin Marietta Energy Systems, Inc. under contract DE-AC05-840R21400 with the U.S. Department of Energy.

be just the Boltzmann equation with a Pauli blocking factor in the collision integral, and is called the Uehling-Uhlenbeck equation. However, the collisional theories must be regarded as tentative, because the assumptions made in their derivation cannot be given firm justification, as will be seen. Also, the evaluation of such theories and comparison with experiment is still in an early stage. In the last year, considerable progress has been made in the numerical solution of the Uehling-Uhlenbeck equation, and the techniques will be described in the last lectures. The physics of the heavy-ion collision looks quite different with and without nucleon-nucleon collisions; even at moderate energies, the collisions tend to bring a rapid approach to local equilibrium in the nuclear medium.

DERIVATION OF MEAN-FIELD THEORY

This lecture will present a derivation of mean-field theory that is readily extended to collisional theories. The starting point is the Hamiltonian which we will assume, for the present, contains only kinetic energy and two-particle interactions. We write the Hamiltonian in second quantized notation as

$$\hat{H} = \sum_{i,j} \langle i \,|\, T \,|\, j \rangle \, a_i^\dagger a_j + \frac{1}{2} \sum_{\substack{i,j \\ k,\ell}} \langle ij \,|\, V \,|\, k\ell \rangle \, a_i^\dagger a_j^\dagger a_\ell a_k . \tag{1}$$

The indices i,j label a convenient complete set of single-particle states. The second quantized formalism is used because it is the easiest way to deal with the antisymmetry of the wavefunction, which will be nontrivial in the later development of the theory. The wavefunction satisfying the Hamiltonian (1) will be denoted by $\psi(t)$; if we knew ψ, the problem would be solved. We shall set ourselves the more modest goal of determining the one-body density matrix, ρ. This is defined by its matrix elements

$$\rho_{ij} = \langle \psi | a_i^\dagger a_j | \psi \rangle \tag{2}$$

The equation of motion for the density matrix is the relation satisfied by its time derivative; this is evaluated using the equation of motion for ψ and ψ^*,

$$\hat{H} | \psi \rangle = i \frac{\partial}{\partial t} | \psi \rangle ; \quad \langle \psi | \hat{H} = -i \partial / \partial t \, \langle \psi | . \tag{3}$$

The result is the usual commutator formula,

$$\begin{aligned} \dot{\rho}_{ij} &= \frac{1}{i} \langle \psi | \left[a_i^\dagger a_j , \hat{H} \right] | \psi \rangle \\ &= \frac{1}{i} \langle \psi | \left[a_i^\dagger , \hat{H} \right] a_j + a_i^\dagger \left[a_j , \hat{H} \right] | \psi \rangle \end{aligned} \tag{4}$$

The commutator of the kinetic energy operator with a creation or annihilation operator is a linear combination of such operators,

$$[a_i, \hat{T}] = \sum_j \langle i \mid T \mid j \rangle \, a_j$$
$$[a_i^\dagger, \hat{T}] = -\sum_j \langle j \mid T \mid i \rangle \, a_j^\dagger \tag{5}$$

The kinetic energy contribution to the equation of motion is then

$$\dot{\rho}_{ij}\Big|_{\text{kinetic}} = \frac{1}{i} \langle \psi | [a_i^\dagger a_j, \hat{T}] | \psi \rangle$$
$$= \frac{1}{i} \langle \psi | -\sum_k \langle k|T|i\rangle \, a_k^\dagger a_j + \sum_k \langle j|T|k\rangle \, a_i^\dagger a_k | \psi \rangle$$
$$= \frac{1}{i} \sum_k \{ \langle j|T|k\rangle \, \rho_{ik} - \langle k|T|i\rangle \, \rho_{kj} \}. \tag{6}$$

Note that the only information required about the wavefunction in Eq. (6) is the single-particle density matrix.

Equation (6) can be simplified further by making a suitable choice of representation. If we use momentum eigenstates for our basis, the kinetic energy will be diagonal, and the density matrix obeys the simple equation,

$$\dot{\rho}_{ij}\Big|_{\text{kinetic}} = \frac{1}{i} \left(\frac{p_j^2}{2m} - \frac{p_i^2}{2m} \right) \rho_{ij} \tag{7}$$

The commutator of the potential with the density operator is more complicated, requiring the expectation value of operator products with quadruple Fock space operators,

$$\langle \psi | [a_i^\dagger a_j, \hat{V}] | \psi \rangle = \frac{1}{2} \sum_{k,\ell,m} (\langle jk|V|\ell m\rangle - \langle kj|V|\ell m\rangle) \langle \psi | a_i^\dagger a_k^\dagger a_m a_\ell | \psi \rangle$$
$$+ \frac{1}{2} \sum_{k,\ell,m} (\langle \ell m|V|ik\rangle - \langle \ell m|V|ki\rangle) \langle \psi | a_\ell^\dagger a_m^\dagger a_k a_j | \psi \rangle$$

At this point, we are ready to derive mean-field theory. The fundamental approximation is to evaluate the expectation of the four-particle operator by a product of single-particle densities,

$$\langle \psi | a_i^\dagger a_j^\dagger a_k a_\ell | \psi \rangle = \langle \psi | a_i^\dagger a_\ell | \psi \rangle \langle \psi | a_j^\dagger a_k | \psi \rangle$$
$$- \langle \psi | a_i^\dagger a_\ell | \psi \rangle \langle \psi | a_j^\dagger a_\ell | \psi \rangle \tag{9}$$
$$= \rho_{i\ell} \rho_{jk} - \rho_{i\ell} \rho_{j\ell}.$$

Equation (7) is the Hartree-Fock approximation to the two-particle density matrix. It is exact if the wavefunction is a Slater determinant of single-particle wavefunctions. The antisymmetry is explicit with the two terms on the right; if k and ℓ are interchanged, the expectation changes sign. The first term alone is the Hartree approximation; it requires that a physical distinction be made between i,ℓ states and j,k states. The approximation is good for treating the two-particle density for particles in widely separated parts of the system if there are no long-range correlations in the wavefunction.

The Hartree-Fock two-particle density matrix cannot be correct for particles close to each other when the interactions are very strong, but it might still serve as a useful approximation if the Hamiltonian is appropriately modified. In that case, the theory will be called the mean-field theory.

Inserting (9) and (6) in Eq. (4) gives a closed equation of motion for the single-particle density matrix. It is convenient to write this in terms of a single-particle potential, U, defined by the matrix elements

$$\langle j|U|\ell\rangle = \sum_{km} \left(\langle jk|V|\ell m\rangle - \langle jk|V|m\ell\rangle\right)\rho_{km} \tag{10}$$

Then the potential interaction commutator is

$$\langle\psi|\left[a_i^\dagger a_j, \hat{V}\right]|\psi\rangle = \sum_k \left(\langle j|U|k\rangle\rho_{ik} - \rho_{kj}\langle k|U|i\rangle\right) \tag{11}$$

and the equation of motion can be expressed in terms of a single-particle Hamiltonian H_{MF}

$$\dot{\rho}_{ij} = \frac{1}{i}\left[\rho_{ik}\langle j|H_{MF}|k\rangle - \langle k|H_{MF}|j\rangle\rho_{kj}\right] \tag{12}$$

where $\hat{H}_{MF} = \hat{T}+\hat{U}$. Equation (12), together with (10), defines the time-dependent Hartree-Fock approximation. There are two particular representations for Eq. (12) that are useful for numerical calculations or for further approximation. The first representation is obtained by expanding the density matrix as a sum over dyadic matrices,

$$\rho_{ij} = \sum_\alpha \left(b_i^\alpha\right)^* b_j^\alpha \tag{13}$$

Then Eq. (12) is solved if the b satisfy

$$\frac{db_j^\alpha}{dt} = \frac{1}{i}\sum_k \langle j|H_{MF}|k\rangle\, b_k^\alpha. \tag{14}$$

In coordinate space, the vector $\sum_j b_j^\alpha |\, j\rangle$ is just the single-particle wavefunction $\phi^\alpha(x)$. The coordinate space representation is especially useful if the potential U is approximated by a local function of position.

Another useful representation uses the Wigner function. This is defined as a certain Fourier transform of the density matrix, starting from either the coordinate space or momentum space representation,

$$f(p,r) = \int d\vec{s}\, e^{ip\cdot s}\, \rho_{r+\frac{s}{2},r-\frac{s}{2}} \qquad (15a)$$

$$f(p,r) = \int \frac{d\vec{q}}{(2\pi)^3}\, e^{-iq\cdot r}\, \rho_{p+\frac{q}{2},p-\frac{q}{2}} \qquad (15b)$$

The Wigner function has all the properties of a classical phase space distribution function while remaining a quantum-mechanical density. For example, the ordinary spatial density is obtained from f by integrating over p,

$$\begin{aligned}\int \frac{d\vec{p}}{(2\pi)^3} f(p,r) &= \int \frac{d\vec{p}}{(2\pi)^3}\, d\vec{s}\, e^{ip\cdot s}\, \rho_{r+\frac{s}{2},r-\frac{s}{2}} \\ &= \int d\vec{s}\, \delta^{(3)}(s)\, \rho_{r+\frac{s}{2},r-\frac{s}{2}} \\ &= \rho_{r,r} = \rho(r).\end{aligned} \qquad (16)$$

It is also easy to show that the expectation of the momentum and kinetic energy are given by the integrals over f:

$$\begin{aligned}\langle \vec{p} \rangle &= \int d\vec{r}\, \frac{d\vec{p}}{(2\pi)^3}\, \vec{p}\, f(\vec{p},\vec{r}) \\ \langle T \rangle &= \int d\vec{r}\, \frac{d\vec{p}}{(2\pi)^3}\, \frac{p^2}{2m}\, f(p,r)\end{aligned} \qquad (17)$$

We now express the mean-field equation of motion in the Wigner representation. This may be done by taking the time derivative of the definition of the Wigner function, Eq. (15), and substituting the equation of motion for $\dot{\rho}$,

$$\frac{df(p,r)}{\partial t} = \frac{1}{i}\int \frac{d\vec{q}}{(2\pi)^3}\, e^{-iq\cdot r}\, [\rho, H_{MF}]_{p+\frac{q}{2},p-\frac{q}{2}}$$

$$= \frac{1}{i}\int \frac{d\vec{q}}{(2\pi)^3}\, e^{-iq\cdot r}\, \{[\rho,\hat{T}] + [\rho,U]\}_{p+\frac{q}{2},p-\frac{q}{2}} \qquad (18)$$

$$= \left.\frac{\partial f}{\partial t}\right|_{\text{kinetic}} + \left.\frac{\partial f}{\partial t}\right|_{\text{potential}}$$

The momentum representation has been used for ρ, which allows the first term in Eq. (18) to be evaluated with Eq. (7),

$$\int \frac{d\vec{q}}{(2\pi)^3}\, e^{-iq\cdot r}\, [\rho,\hat{T}]_{p+\frac{q}{2},p-\frac{q}{2}} = -\int \frac{d\vec{q}}{(2\pi)^3}\, e^{-iq\cdot r}\, \frac{p\cdot q}{m}\, \rho_{p+\frac{q}{2},p-\frac{q}{2}} \qquad (19)$$

The factor $\vec{q}\, e^{-iq\cdot r}$ in the above integral is replaced by $i\vec{\nabla}_r\, e^{-iq\cdot r}$. Next, the gradient operator is moved outside of the integral, leaving an integral which is proportional to the Wigner function,

$$\left.\frac{\partial f}{\partial t}\right|_{\text{kinetic}} = -\int \frac{d\vec{q}}{(2\pi)^3}\, e^{-iq\cdot r}\, \frac{p\cdot\nabla_r}{m}\, \rho_{p+\frac{q}{2},p-\frac{q}{2}}$$

$$= -\nabla_r \cdot \int \frac{d\vec{q}}{(2\pi)^3}\, e^{-iq\cdot r}\, \frac{\vec{p}}{m}\, \rho_{p+\frac{q}{2},p-\frac{q}{2}} \qquad (20)$$

$$= -\nabla_r \cdot \frac{p}{m}\, f(p,r)$$

The second term in Eq. (18) can only be simplified under restricted assumptions. Let us first assume that the mean-field potential is local in coordinate space

$$\langle \vec{r}\,|\, U\,|\, \vec{r}' \rangle = \delta(\vec{r}-\vec{r}')\, U(\vec{r}) \qquad (21)$$

In general, this is not true for the exchange potential. It will be true if the interaction is zero range, and it is a reasonable approximation in any case. The effects of the nonlocality can be incorporated into the theory in other ways, such as with the effective mass, which will not be discussed in these lectures. The potential term in Eq. (18) is evaluated in the coordinate space representation, using Eq. (21),

$$\left.\frac{\partial f}{\partial t}\right|_{\text{potential}} = -\frac{1}{i}\int ds^{+}\, e^{ip\cdot s}\left(U(r+\tfrac{s}{2}) - U(r-\tfrac{s}{2})\right)\rho_{r+\frac{s}{2},r-\frac{s}{2}} \tag{22}$$

The lefthand side can be expressed in terms of the Wigner function by using the inverse Fourier transform of Eq. (15a), and the result is an integral over the Wigner function for all values of p. With one additional approximation, the theory simplifies much further. We assume that U is a sufficiently smoothly varying function of r to permit truncation of the Taylor series for the U factor by the lowest nonvanishing term,

$$U(r+s)-U\left(r-\tfrac{s}{2}\right) = s\cdot\nabla_r U \tag{23}$$

We insert this in Eq. (22) and use the same trick to convert the s factor in the integrand to a gradient which can be taken out of the integral. The result is identical to the potential term in the classical Liouville equation for the single-particle distribution function in the field U. The final equation is that Liouville equation,

$$\frac{\partial}{\partial t} f + \frac{p}{m}\cdot\nabla_r f - \nabla_r U\cdot\nabla_p f = 0 \tag{24}$$

With U the self-consistent field associated with f, Eq. (24) is known as the Vlasov equation. It is remarkable that quantum physics only plays a role in the initial conditions on f. The initial f must respect the Pauli principle, e.g. be based on a Slater determinantal many-particle wavefunction. In ground state wavefunctions, f will be close to 1 in occupied regions of phase space and close to zero outside. But the identity of the particles plays no role beyond the initial conditions.

Conservation Laws

Conservation laws are very important in areas of physics for which the dynamic equations are difficult to solve. When one develops a simplified theory in such areas, the requirement that the theory respect the conservation laws is often sufficiently stringent to be helpful in formulating the theory. For the physics of heavy-ion collisions, the most important conservation laws are for particle number, momentum, and energy. Mean-field theory passes the test of satisfying these conservation laws. This is easy to show for the case of particle number, which is defined in the three representations as

$$N = \sum_i \rho_{ii} = \sum_\alpha \int d^3r\, \phi_\alpha^*(r)\phi_\alpha(r) = \int \frac{d^3p}{(2\pi)^3}\, d^3r\, f(p,r) \tag{25}$$

The proof that N is conserved proceeds by taking its time derivative and evaluating the righthand side using the equation of motion. In

the density matrix representation, this yields

$$\frac{dN}{dt} = \sum_i \delta_{ii} = \frac{1}{i} \left[H_{MF}, \rho\right]_{ii} = 0 \tag{26}$$

The last step follows by the symmetry of the commutator. In the particle wavefunction representation, the conservation law proof relies on the Hermitian character of H_{MF},

$$\frac{dN}{dt} = \frac{1}{i} \sum_\alpha \int d^3r \left[\phi_\alpha^* H_{MF} \phi_\alpha - \phi_\alpha H_{MF} \phi_\alpha^*\right] = 0 \tag{27}$$

Finally, in the Wigner representation, the conservation law is

$$\begin{aligned} \frac{dN}{dt} &= \int \frac{d^3p}{(2\pi)^3} d^3r \left[-\frac{p}{m} \cdot \nabla_r f + \nabla_r U \cdot \nabla_p f\right] \\ &= -\int \frac{d^3p}{(2\pi)^3} \int f \frac{p}{m} \cdot d^2r + \int d^3r \int \frac{f}{(2\pi)^3} \nabla_r U \cdot d^2p = 0 \end{aligned} \tag{28}$$

with the last step obtained by evaluating the surface integrals at a large distance or momentum, where f=0.

The conservation law for momentum depends on the translational invariance of the potential interaction in the Hamiltonian. We made certain approximations in the treatment of the interaction when we derived mean-field theory. The theory will conserve momentum as long as those approximations preserve translational invariance. To illustrate this, let us assume a generalized interaction,

$$\begin{aligned} \hat{V} = \frac{1}{2} \int d^3r \, d^3r' \, \hat{\rho}(r)\hat{\rho}(r') \, v_2(r,r') \\ + \frac{1}{3} \int d^3r \, d^3r' \, d^3r'' \, \hat{\rho}(r)\hat{\rho}(r')\hat{\rho}(r'')v_3(r,r',r'') + \ldots \end{aligned} \tag{29}$$

Neglecting exchange terms, the mean field associated with the above interaction is

$$\begin{aligned} U(r) = \frac{1}{2} \int d^3r' \, \rho(r')\left(v_2(r,r')+v_2(r',r)\right) \\ + \frac{1}{3} \int d^3r' \, d^3r'' \, \rho(r')\rho(r'')\left(v_3(r,r',r'')+v_3(r',r,r'')\right. \\ \left. + v_3(r',r'',r)\right) + \ldots \end{aligned} \tag{30}$$

We now examine the equation of motion for the total momentum. In the particle wavefunction representation this is

$$\frac{d\vec{p}}{dt} = \frac{d}{dt}\sum_\alpha \int d^3r\ \phi_\alpha^*\ \left[\frac{\vec{\nabla}-\vec{\nabla}}{2i}\right]\phi_\alpha$$

$$= \frac{1}{i}\sum_\alpha \int d^3r\ \phi_\alpha^* \left\{\left[\frac{\vec{\nabla}-\vec{\nabla}}{2i},\ T\right] + \left(\frac{\vec{\nabla}-\vec{\nabla}}{2i},\ U\right)\right\}\phi_\alpha \tag{31}$$

The commutator of the momentum operator with the kinetic energy vanishes, and the commutator with U is proportional to the gradient of U,

$$\frac{d\vec{p}}{dt} = -\int d^3r\ \rho(r)\ \vec{\nabla}_r U \tag{32}$$

Translational invariance of the interaction implies that

$$(\nabla_r + \nabla_{r'} + \ldots)v_m(r,r',\ldots) = 0 \tag{33}$$

The integral in Eq. (32) can be shown to vanish using Eqs. (30) and (33).

The mean-field theory with the generalized interaction Eq. (29) also conserves energy. To prove this, we start by expressing the energy as the expectation of the Hamiltonian, using the mean-field density matrix and neglecting exchange terms,

$$E = \sum_\alpha \int d^3r\ \phi_\alpha^*\, T\phi_\alpha + \frac{1}{2}\int d^3r\ d^3r'\ \rho(r)\rho(r')v_2(r,r') + \frac{1}{3}\int \ldots. \tag{34}$$

The equation of motion for E becomes

$$\frac{dE}{dt} = \frac{1}{i}\sum_\alpha \int d^3r\ \phi_\alpha^*[T,H_{MF}]\phi_\alpha + \int d^3r\ d^3r'\ \delta(r)\rho(r')v_2(r,r') + \int \underbrace{d^3r\ d^3r'\ d^3r''\ldots}_{\int d^3r\ \delta(r)\ U(r)} \tag{35}$$

The second and later terms in this equation can be combined, and the coefficient δ is equal to the mean field. Finally, δ is evaluated by the equation of motion, yielding

$$\frac{dE}{dt} = \frac{1}{i}\sum_\alpha \int d^3r\ \phi_\alpha^*\ [T,H_{MF}]\phi_\alpha + \frac{1}{i}\sum_\alpha \int d^3r\ \phi_\alpha^*\ [U,H_{MF}]\phi_\alpha$$

$$= \frac{1}{i}\sum_\alpha \int d^3r\ \phi_\alpha^*\ [H_{MF},H_{MF}]\phi_\alpha = 0 \tag{36}$$

Having disposed of the global conservation laws, we now inquire about the existence of local conservation laws, in which the density of a conserved quantity is related to its flux. In that form the conservation laws are of quite direct value, because one of the objects of theory is to calculate the transport of the various conserved quantities from one nucleus to another. To establish a local conservation law, we first define the density whose integral is the globally conserved quantity

$$Q = \int d^3r \; q(r) \tag{37}$$

Then a local conservation law will exist if a current $\vec{j}(r)$ can be found so that the equation of continuity is satisfied,

$$\frac{\partial q}{\partial t} + \vec{\nabla}\cdot\vec{j} = 0 \tag{38}$$

In the law for the conservation of the number of particles, the density and current have their usual quantum-mechanical definitions,

$$\rho(r) = \sum_\alpha \phi_\alpha^* \, \phi_\alpha \tag{39}$$

$$\vec{j}(r) = \sum_\alpha \phi_\alpha^* \left(\frac{\vec{\nabla}-\vec{\nabla}}{2im}\right)\phi_\alpha(r) = \int \frac{d^3p}{(2\pi)^3}\,\frac{\vec{p}}{m}\, f(p,r) \tag{40}$$

The equation of continuity is easily derived from the equation of motion for ρ. The local conservation law for momentum is less obvious. The momentum density is defined by

$$\vec{p}(r) = m\vec{j}(r), \tag{41}$$

and the momentum flux will be determined from the equation of motion. Evaluating the time derivative of $\vec{p}(r)$ in the usual way, we find

$$\frac{\partial \vec{p}(r)}{\partial t} = \frac{1}{i}\sum_\alpha \left[\phi_\alpha^* \left(\frac{\vec{\nabla}-\vec{\nabla}}{2i}\right) H_{MF}\phi_\alpha - \left(H_{MF}\phi_\alpha^*\right)\left(\frac{\vec{\nabla}-\vec{\nabla}}{2i}\right)\phi_\alpha\right] \tag{42}$$

$$= -\nabla_\mu \cdot \sum_\alpha \phi_\alpha^* \left(\frac{\vec{\nabla}-\vec{\nabla}}{2}\right)\left(\frac{\vec{\nabla}-\vec{\nabla}}{2m}\right)_\mu \phi_\alpha^* - \rho(r)\,\vec{\nabla}U(r) \tag{43}$$

Only the first term in Eq. (43) has the required form as a divergence of a vector. The second term can be manipulated into the proper form under certain assumptions. If the interaction is short range compared to the scale of variation of the density, then U(r) may be taken to depend only on the density at r, i.e. $U(r) = U(\rho(r))$. The potential energy is then expressible as an integral over the potential energy density given by

$$V(r) = \int_0^{\rho(r)} d\rho\, U(\rho) \tag{44}$$

We now define the tensor

$$\overleftrightarrow{W} = \delta_{\mu\nu}(\rho U - V) \tag{45}$$

and evaluate its divergence

$$\vec{\nabla}\cdot\overleftrightarrow{W} = \vec{\nabla}(\rho U - V) = U\vec{\nabla}\rho + \rho\vec{\nabla}U - \vec{\nabla}\int_0^{\rho(r)} d\rho\, U(r) = \rho\vec{\nabla}U.$$

This is just the second term in Eq. (43) showing that the required momentum flux from the potential interaction is given by (45). The total momentum current is then

$$\Pi_{\mu\nu} = \Pi_{\mu\nu}^{\text{particle}} + \delta_{\mu\nu}(\rho U - V) \tag{46}$$

where Π^{particle} is the particle contribution to the momentum flux,

$$\begin{aligned}\Pi_{\mu\nu}^{\text{particle}} &= -\sum_\alpha \phi_\alpha^* \left(\frac{\vec{\nabla}-\vec{\nabla}}{2}\right)_\mu \left(\frac{\vec{\nabla}-\vec{\nabla}}{2m}\right)_\nu \phi_\alpha \\ &= \int \frac{d^3p}{(2\pi)^3} \frac{p_\mu p_\nu}{m} f(p,r).\end{aligned} \tag{47}$$

In the next lecture, Eq. (46) will be applied to the calculation of momentum transfer between colliding nuclei.

Effective Hamiltonians

Because of the strength and spin dependence of the interaction, mean-field theory cannot be applied directly to the nuclear Hamiltonian. Correlations are induced between the particles at short distances which may be important for a fundamental understanding of nuclear properties but which play a minor role in the physics at low excitation energies. In principle, there are theories such as the Brueckner theory that allow one to derive an effective mean-field description starting from a fundamental interaction. However, this program has not been entirely successful; the predicted binding energy and nuclear matter density are not in agreement with the empirical saturation properties. The present-day philosophy is to bypass the steps to get from a fundamental interaction to an effective mean field and simply postulate an effective Hamiltonian which satisfies the known empirical requirements. Some guidance as to the form of the effective Hamiltonian comes from many-particle perturbation theory which expresses the binding energy (per particle) as a power series in the Fermi momentum or the cube root of the density,[1]

$$\begin{aligned}E &= ak_F^2 + bk_F^3 + ck_F^4 + \ldots \\ &= a'\rho^{2/3} + b'\rho + c'\rho^{4/3} + \ldots\end{aligned} \tag{49}$$

The first term is the kinetic energy of a free Fermi gas having the coefficient $a = 3/5\ h^2/2m$. The second and higher terms are due to potential interactions and correlations. The main empirical constraints on the function (49) are that it have a minimum at $\rho = 0.17$ fm or $k_F = 1.34$ fm, and that the binding energy at the minimum be $E = -15$ MeV. Another constraint that may be invoked is that the compressibility coefficient of nuclear matter be consistent with the empirical vibrational frequency of the giant monopole vibration. Having three conditions to satisfy, the next two terms in the power series expansion are overdetermined. We can make a three-parameter potential model by using the power of ρ as a free parameter in the third term. Thus, we consider a mean field of the form

$$U(\rho) = A\rho + B\rho^{\sigma} \tag{50}$$

The associated potential energy density is

$$V(\rho) = \frac{1}{2} A\rho^2 + \frac{1}{\sigma+1} B\rho^{\sigma+1} \tag{51}$$

The choice $\sigma=2$ gives a density-dependent mean field that can be directly associated with a potential of the form Eq. (29). The proper compressibility is obtained for a choice $\sigma=7/6$. The two mean-field functions are

$$\begin{aligned} \text{Stiff:}\quad & U(\rho) = -124\ (\rho/\rho_o) + 70.5\ (\rho/\rho_o)^2 \text{ MeV} \\ \text{Soft :}\quad & U(\rho) = -356\ (\rho/\rho_o) + 303\ (\rho/\rho_o)^{7/6} \text{ MeV} \end{aligned} \tag{52}$$

The designations stiff and soft refer to the compressibility coefficients which are K=380 MeV and K=200 MeV, respectively. In Figs. 1 and 2 are plotted the binding energy and the mean field associated with these two functions. Figure 1 shows that the functions reproduce the proper binding energy and saturation density. The two functions are quite similar at subnuclear densities and only differ substantially at strong compressions. The mean field is close to -50 MeV for both functions at normal density, in agreement with other kinds of empirical information about the potential. Notice that the soft function is rather flat at higher-than-normal densities. This observation will simplify the discussion of the compressed matter dynamics.

Heavy-Ion Collisions in Mean-Field Theory

The dominant physics of close collisions between nuclei is associated with the mutual exchange of particles between the nuclei. Nucleons pass freely from one nucleus to the other when they come together. Particularly with the soft potential field, the field does not change very much in the overlap region and the motion of the

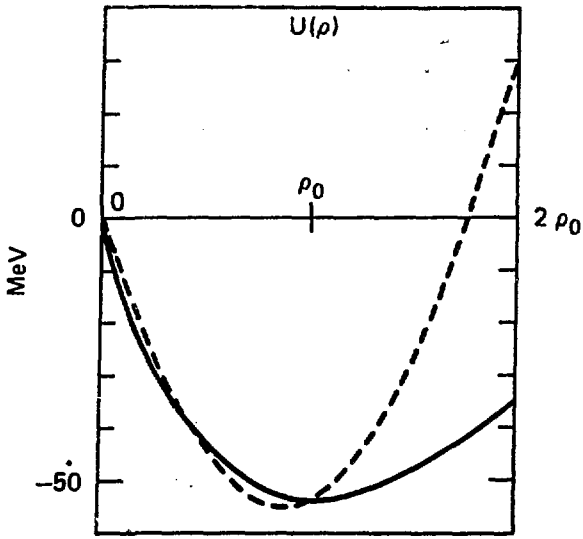

Fig. 1. Mean-field potential U(ρ) for the two functions of Eq. (52). The soft and stiff potential functions are shown by dashed and solid lines, respectively.

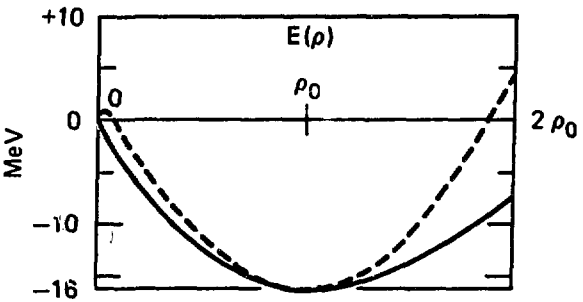

Fig. 2. Energy per nucleon as a function of density. The soft and stiff functions are shown by dashed and solid lines, respectively.

nucleons is only affected by the external surfaces of the two nuclei. The evolution of the density matrix is shown schematically in terms of the Wigner function in Fig. 3. The dependence of f on the longitudinal coordinate and momentum is shown with the shaded areas representing regions with $f \cong 1$. Of course, the actual Wigner function will have smooth variation instead of the sharp boundaries sketched. The boundaries in coordinate space represent the physical surfaces of the nuclei; the momentum boundaries are at the Fermi momentum. Since

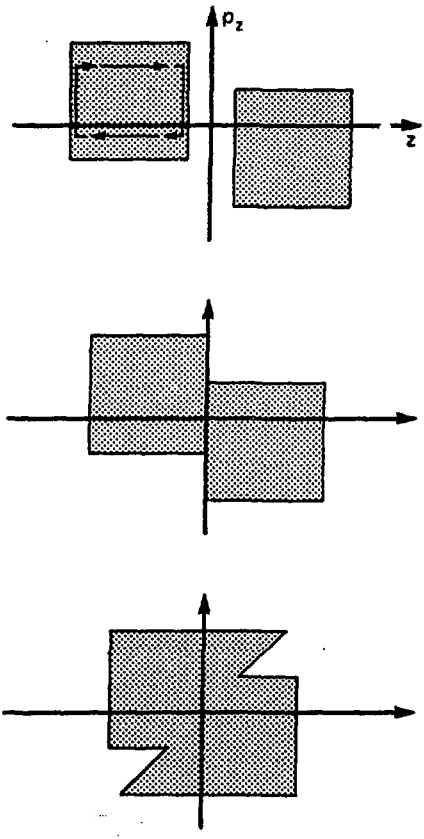

Fig. 3. Schematic picture of phase space distribution of nucleons in two colliding nuclei. From the top down, picture shows distribution before, at, and after the nuclei come into contact.

the nuclei are moving toward each other, the distribution functions for each nucleus have a displacement in momentum. In the classical picture of the motion, particles are moving within the phase space boundaries and are reflected at the nuclear surface to stream in closed loops, as shown by the arrows. Once the nuclei touch, there is no inner surface to reflect from, and the nucleons pass over to the other side. This is indicated in the lower two drawings.

The qualitative physics described here is born out quite well by numerical studies of the quantum and the classical mean-field theories.[2,3] In Fig. 4 is shown the comparison of one-dimensional TDHF with the corresponding Vlasov theory from Ref. 3. The two

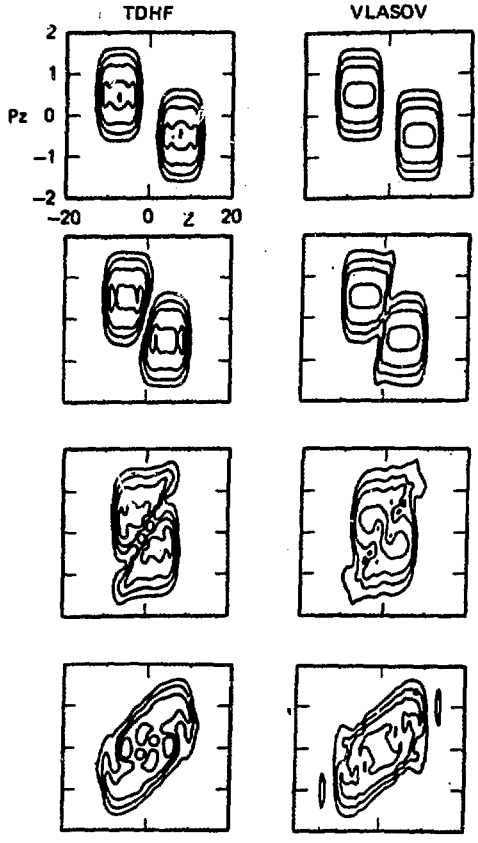

Fig. 4. Comparison of TDHF and Vlasov equation for the evolution of the phase space distribution function in one dimension, from Ref. 3.

theories are very similar, with the only qualitative difference from the schematic picture of Fig. 3 being the presence of a hole at p=0 and r=0.

For three-dimensional geometry, the quantum mean-field theory is quite difficult numerically, but enough calculations have been done to survey the range of collision conditions possible. Some reviews of the theory and comparison with experiment are given in Refs. 4 and 5. In general, the theory is successful in describing the energy and momentum transfer at low energies. Because of the difficulty in

Reduction of Mean-Field Theory to Force Dynamics

Because of the difficulty in treating three-dimensional aspects

realistically, it is useful to consider simplified treatments. A semiquantitative description of the mean-field dynamics can be developed by approximating the momentum flux tensor. This can be evaluated at the contact surface between the nuclei to calculate the momentum transfer. Since the rate of momentum transfer is a force, we will have a theory for forces between nuclei in close contact. We begin by choosing a plane to divide space into two regions and define the conserved quantities associated with each nucleus by integrating over the appropriate region of space. Labeling the regions A and B, the momentum, position, and number of nucleons in nucleus A are given by

$$\begin{aligned} \vec{p}_A &= \int_A d^3r\ \vec{p}(r) = \sum_\alpha \int_A d^3r\ \phi_\alpha^* \left(\frac{\vec{\nabla}-\vec{\nabla}}{2i}\right)\phi_\alpha \\ \vec{r}_A &= \int_A d^3r\ \vec{r}\rho(r) \\ N_A &= \int_A d^3r\ \rho(r). \end{aligned} \tag{53}$$

The equations of motion for r_A and p_A may now be determined using the local conservation laws. Taking the time derivative of the equation for r_A, we replace ∂ by the negative divergence of the current. The divergence can be integrated by parts, giving a surface integral which vanishes if we choose the dividing plane so that

$$\frac{dN_A}{dt} = 0 \tag{54}$$

The result is the familiar equation

$$\frac{d\vec{r}_A}{dt} = \frac{\vec{p}_A}{m} \tag{55}$$

The force equation is obtained from a similar set of manipulations,

$$\frac{d\vec{p}_A}{dt} = \int dS \cdot \Pi \tag{56}$$

Since the momentum flux could only be defined for short-range interactions, Eq. (56) does not contain the Coulomb interaction, which must be added separately. Note that Eq. (56) is in the form of a surface integral on the area of contact between the two nuclei. This form is convenient and physically sensible for discussing the macroscopic force dynamics. We next evaluate the pressure tensor Π using macroscopic limits. In infinite nuclear matter, the particle flux contribution to the pressure can be calculated from the geometry of the Fermi surface. If the potential field remains constant in the colliding nuclei, the Fermi surface will be in the shape of two intersecting Fermi spheres centered at the momenta of the two nuclei. The overlap region of the two spheres has the same density as the other parts of the distribution—refer to Fig. 3 to see how the

nucleon distributions merge without violating the Pauli principle. The particle momentum flux for the intersecting sphere geometry was calculated by Randrup[11] who keeps the lowest terms in a power series in the relative momentum of the spheres. The result is

$$\Pi_{\mu\nu}^{\text{particle}} \cong \delta_{\mu\nu}\cdot\text{constant} + \frac{3}{16}\rho_o v_F m \left(\vec{v}_A-\vec{v}_B\right)_\mu \hat{n}_\nu + \hat{n}_\mu\left(\vec{v}_A-\vec{v}_B\right)_\nu \tag{57}$$

where $\hat{n}$ is the normal to the dividing surface, and v_F is the Fermi velocity. The case $v_A-v_B=0$ should represent nuclear matter in equilibrium, which has zero pressure. Thus the constant term in Eq. (57) must be cancelled by the potential contribution to the pressure at normal nuclear matter density. The cancellation will not be perfect for nonzero relative velocities. However, for the soft potential function, the potential contribution is small and Eq. (57) is a reasonable approximation to the entire momentum flux.

The infinite matter Fermi gas approximation will break down near the surface of a nucleus. In fact, the pressure tensor is nonzero in the surface even for nuclear matter in equilibrium, giving rise to the surface tension. Rather than treat the full quantum mechanics of the density matrix in the surface region, we shall adopt a macroscopic description, and augment the bulk momentum flux with a surface contribution. The empirical surface tension, σ=1 MeV/fm^2, fixes the integral of the pressure tensor across the surface. We shall describe the contact area of the two nuclei as a circle of radius R_n, which reduces the dynamic equation to

$$\frac{d\vec{p}_A}{dt} = \pi R_n^{\,2}\frac{3}{16}\rho_o v_F m\left(\left(\vec{v}_A-\vec{v}_B\right) + \hat{n}\left(\vec{v}_A-\vec{v}_B\right)\cdot\hat{n}\right) + 2\pi R_n\sigma$$
$$+ \text{Coulomb interaction} \tag{58}$$

The solution of this equation requires knowledge of the evolution of R_n and of the relative velocities of the Fermi spheres. Randrup makes the assumption that the Fermi sphere velocity is equal to the instantaneous velocity of the nuclear centers of mass, $v_{A,B}=\dot{r}_{A,B}$. This results in a linear friction force. The situation is more complicated in mean-field physics. The velocity of the Fermi sphere is determined by the physical surface velocity at the points where the particles in question changed direction. There is a time delay of the order of the nuclear transit time before these particles reach the contact zone. The motion of the farther nuclear surfaces is additionally delayed with respect to the center-of-mass motion. Thus, in mean-field physics a better description of the velocity of the Fermi surfaces is to relate it to the center-of-mass velocity at an earlier time,

$$\left(v_A-v_B\right)_f \approx \left(\dot{r}_A-\dot{r}_B\right)_{t-\tau_D} \tag{59}$$

with the delay time τ_D having the order of magnitude

$$\tau_D \sim (1\text{-}2) \cdot \frac{2R}{v_F} \tag{60}$$

where R is the radius of one of the nuclei. Let us estimate this numerically for medium heavy nuclei. Typical parameters are R~5 fm, v_F~1/4 c, giving

$$\tau_D \sim (1\text{-}2) \cdot \frac{(2)(5\ \text{fm})}{1/4\ c} \sim 40\text{-}80\ \text{fm/c} \tag{61}$$

We next consider the evolution of the contact zone or neck region between the two nuclei. In typical TDHF collisions, the neck forms quickly once the nuclei touch, and grows in size to a substantial fraction of a nuclear radius. If the nuclei come apart again, due to the Coulomb or the centrifugal forces, the neck becomes elongated and shrinks rather slowly in size. This is illustrated by a TDHF calculation, shown in Fig. 5 from Ref. 12, of a collision between two Pb nuclei. The nuclei touch when they approach within 14 fm of each other. The neck grows to about 5.5 fm radius at the distance of closest approach, and then shrinks at about 1/3 of the rate at which the nuclei draw apart.

These features were put in a completely geometric description of the neck radius by A. Bonasera.[6] It is then possible to make a self-contained model for the mean-field collisions. A comparison of the mean-field dynamics and the macroscopic model is shown in Fig. 6,

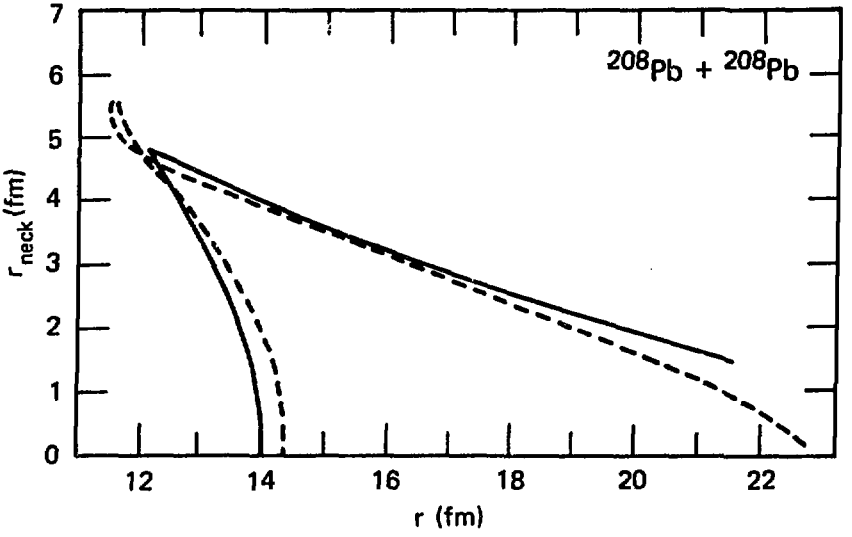

Fig. 5. Neck evolution in TDHF[12] compared with geometric model of Ref. 6.

with the relative velocity of the two nuclei plotted as a function of separation. The nuclei approach with a negative velocity and are slowed down by the Coulomb force. Between 7 and 9 fm separation, the nuclear potential attraction becomes significant, impeding the deceleration. At 7 fm separation, the nuclei touch, and particle transfer becomes important. The associated repulsive force rapidly reduces the velocity to zero. In fact, there is an overshoot, and the nuclei slightly rebound. For the particular collision conditions in Fig. 6, the two nuclei remain fused. If the memory effect in the particle momentum flux is eliminated in favor of a linear friction, the collision does not show a rebound.

Observables

As mentioned earlier, mean-field theory is very successful in describing the main features of low-energy collisions associated with energy loss and momentum transfer. Let us first consider the case of complete momentum transfer, i.e. fusion of the two nuclei. As a function of impact parameter and initial energy, there will be a domain of fusion, which may be defined operationally by requiring that the system hold together for a certain (finite) length of time. Such a fusion region is shown in Fig. 7. There are three distinct physical processes determining the boundaries of fusion. For moderately charged nuclei and low energies and angular momentum, the physics is very simple. If the nuclei surmount the potential barrier of the combined Coulomb and external nuclear potentials, they touch and the attractive force from the surface tension in the neck holds them together. The low energy edge of the fusion domain is determined by this potential barrier physics. At larger impact parameters and therefore higher angular momenta, the centrifugal force is larger than the attraction from the surface tension, and the nuclei scission by a process of elongation and thinning out the neck. For a fixed geometry, the balance of forces occurs at a critical angular momentum,

$$\hbar^2 \ell^2 / \mu r^3 \approx 2\pi R_N \sigma \qquad (62)$$

For the example in the figure, appropriate parameters are $r \sim 6$ fm, $R_n \sim .5$ fm, giving $\ell \sim 35\hbar$. The scission boundary from TDHF actually occurs at this value of the angular momentum. That angular momentum is also close to the maximum angular momentum sustainable in a liquid drop of nuclear matter of that size. Indeed, we see that the only physics that is important for the scission in the mean-field treatment, namely the surface tension and the inertia, is also present in the liquid-drop model. The third boundary in Fig. 7, at small impact parameter and high energy, is known as the fusion window. Physically, the nuclei flow through each other under these conditions, and the attractive bulk forces are insufficient to hold them together in the end. In the macroscopic description, this comes about because of the memory effect in the particle momentum flux. This

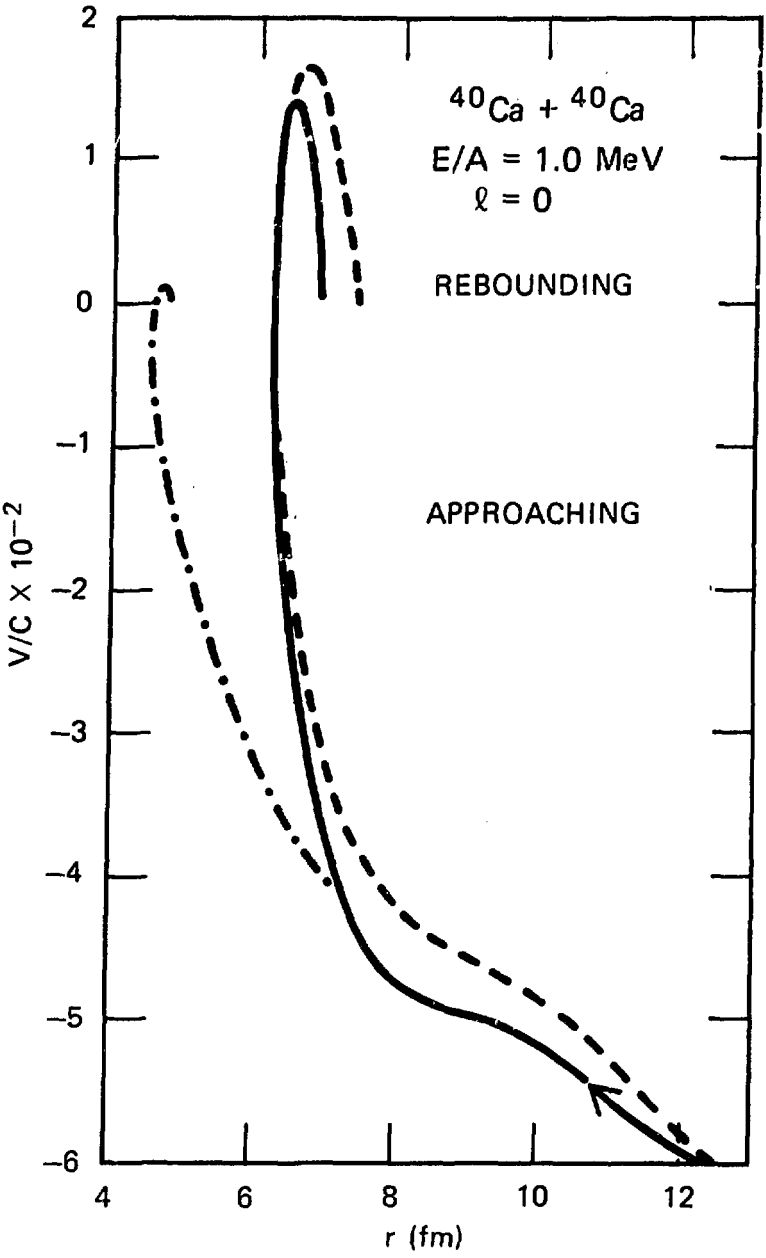

Fig. 6. Relative velocity of collision partners as a function of separation distance. Dashed line shows a TDHF calculation, and solid line shows the simulation by macroscopic force dynamics.[8] The dot-dashed line shows the evolution when the delay time τ_D is set to zero.

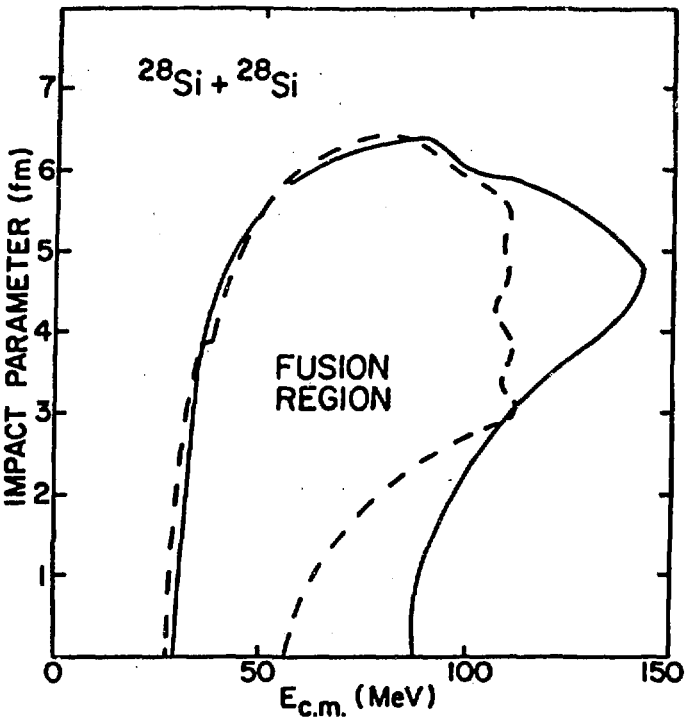

Fig. 7. Fusion region in collisions of $^{28}Si + ^{28}Si$. The dashed boundary is the TDHF result,[7] and the solid line is the simulation by macroscopic force dynamics.[6]

contribution to the force is strongly repulsive, because of the high velocity of the nuclei. The force persists for a significant time after the centers of mass have been brought to rest, so the nuclei begin to separate with a substantial velocity. The Fermi surface of the combined spheres is then smaller than an individual sphere and the density falls below nuclear matter density in the neck's region. The pressure tensor becomes negative, i.e. there is an attractive force between the two nuclei. However, there is a maximum sustainable negative pressure in nuclear matter, the tensile strength. When this is exceeded, the neck will break up into regions of nuclear matter density separated by void regions. We call this mechanism neck snap. However, the macroscopic treatment does not describe this boundary of TDHF as well as the other boundaries. Since the nuclear matter is under a stress extreme here, the details of the Hamiltonian should play some role.

Recently, Davies and collaborators made a study of the fusion window threshold with a number of Hamiltonians, and found a

substantial dependence.[8] The biggest variation was with the Hamiltonians Skyrme II and IV, which gave thresholds of 62.5 MeV and 42.5 MeV, respectively for the window in collisions between ^{16}O nuclei. It should be possible to understand these differences in terms of the properties of the pressure tensor with the various interactions, but so far this has not been done.

On the experimental side, the measured fusion cross sections in medium heavy systems agree with the mean-field theory at low energies. An example is shown in Fig. 8. The cross section increases with energy until the scission begins at the critical angular momentum. The window should cause a more dramatic decrease at higher energies, but so far this has not been observed. The fusion window may well be nonexistent, in which case the mean-field theory would be limited in validity to the lowest energies. An inadequacy of mean-field theory also is found for very light systems, such as $^{12}C + ^{12}C$, where there are pronounced wiggles in the fusion excitation function. These are manifestations of resonances or other quantum effects that are not contained in the mean-field description.

For heavy systems, the Coulomb force becomes significant in determining the fusion boundary. The scission boundary moves down as the charge increases, and at some point it extends to zero impact

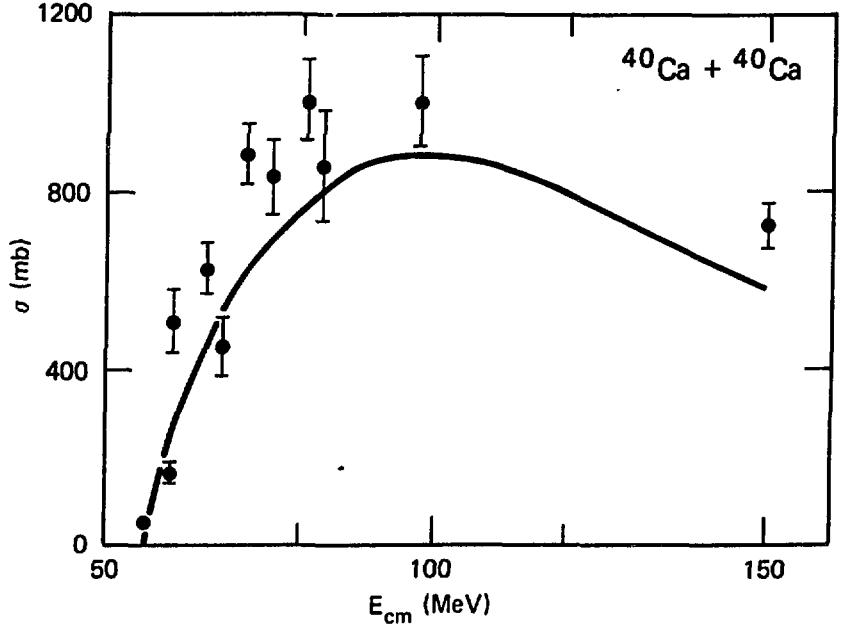

Fig. 8. Experimental fusion cross section in collisions of $^{40}Ca + ^{40}Ca$, compared with macroscopic force model.[6] Experimental data are from Refs. 9 and 8.

parameter. We illustrate this with the macroscopic calculation for $^{120}Sn + ^{120}Sn$ shown in Fig. 9. The fusion boundary has a higher threshold than the potential barrier, which may be understood quite simply. After the nuclei surmount the barrier, they are accelerated toward each other by the external nuclear field. This force can be quite strong; in the proximity model it has a maximum magnitude

$$F_{proximity} \sim 2\pi R\sigma \tag{63}$$

As soon as the nuclei touch the repulsive particle exchange comes into play. The net nuclear force at that time is the surface tension force,

$$F_{surface} \sim 2\pi R_N\sigma \tag{64}$$

which we see is always less than the proximity force. Nuclei are eager to touch each other, but less enthusiastic to remain bonded.

For the more highly charged systems, the net force will be attractive only if the neck exceeds a certain radius, requiring additional bombarding energy above the barrier. This dynamic fusion threshold was first described by Nix and Sierk;[13] Swiatecki gives it the name "extra push". An example is the system $^{209}Bi + ^{54}Cr$, shown in Fig. 10. The experimental data show that the nuclei react with each

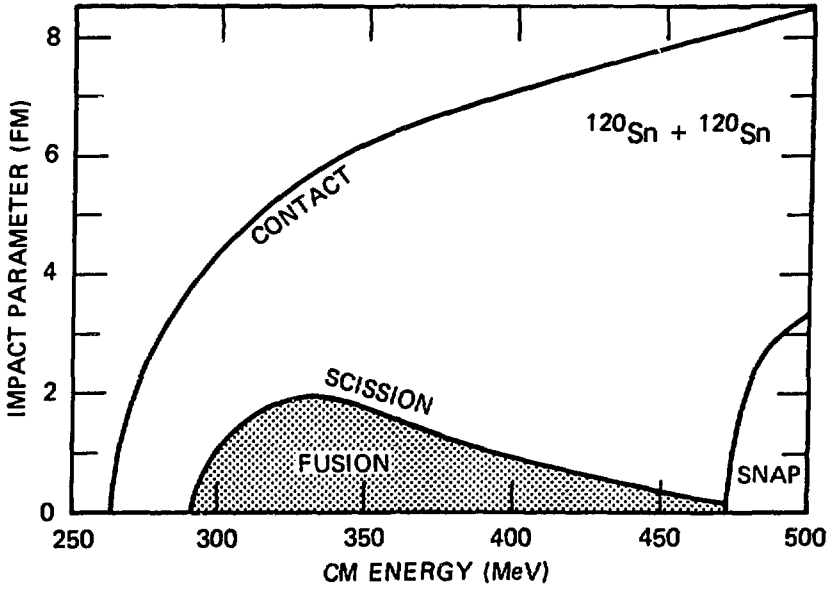

Fig. 9. Fusion region in $^{120}Sn+^{120}Sn$ collisions showing the dynamic fusion threshold.

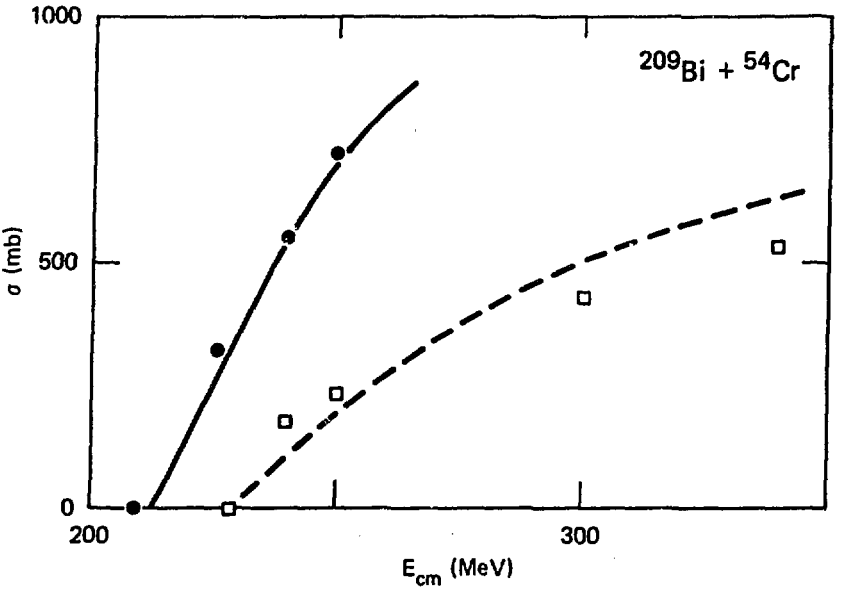

Fig. 10. Reaction cross section and fusion cross section for $^{209}Bi + ^{54}Cr$. The prediction of the macroscopic mean-field model is shown as solid and dashed lines respectively.

other starting at an energy of about 210 MeV, but do not begin to fuse until 230 MeV or so. As with the fusion window, the precise value of the dynamic fusion barrier seems to depend quite sensitively on the nuclear Hamiltonian. Davies et al. found that in one system, $^{84}Kr + ^{139}La$, the barrier varied from 410 MeV to 660 MeV with Hamiltonians ranging from Skyrme III to Skyrme II, respectively.[8] Again, there is no understanding of how the specific characteristics of the Hamiltonians affect the threshold.

Other aspects of low energy collisions that should be mentioned are energy loss and angular distributions of deep inelastic scattering, which are well described by mean-field theory. The deep inelastic scattering is contained in the region between the barrier curve and the scission curve. Because the neck shrinkage rate is low, much energy is lost from the center-of-mass motion. The angular distribution is sensitive to the temporal description of the elongation process; the fact that angular distributions are qualitatively reproduced shows that mean-field theory has about the right time dependences. However, these data also show features that are beyond the possibility to describe in mean-field theory. Namely, there are broad dispersions in angle and in energy, while mean-field theory predicts a unique angle and energy for each impact parameter. There

are a number of ways to go beyond mean-field theory to describe fluctuations. A recent theory of Balian and Veneroni,[14] for example, treats fluctuations associated with neighboring mean fields. More commonly, a theoretical framework is adopted in which the Hamiltonian is separated into a center-of-mass term, an internal term, and a coupling that is treated in some approximate way.

BEYOND MEAN FIELD: NUCLEON-NUCLEON COLLISIONS

At higher energy, mean-field theory gives a poor description of the single-particle density matrix because of the collisions between particles. The central approximation of mean-field theory, Eq. (9), must be replaced by something better. A natural way to approach this task is to use mean-field theory as a starting point and improve the wavefunction with perturbation theory. From a notational point of view, the perturbation development with the full two-particle interaction is cumbersome, so we will start with a simpler problem, developing the perturbations due to a one-particle external field. The generalization to two-particle interactions is merely a question of putting the extra particle operators into the equations.

Perturbation theory begins with a separation of the Hamiltonian into a part which can be solved exactly, H_o, and the remainder V, the perturbation. As mentioned above, we take H_o to be the mean-field Hamiltonian. The unperturbed states are the eigenstates of that Hamiltonian (which change in time) and the multiparticle states built out of those eigenstates. We shall use these states for a basis and assume that the unperturbed density matrix is diagonal,

$$\langle \psi \left| a_i^\dagger a_j \right| \psi \rangle = \rho_{ij} = \delta_{ij} n_i \tag{65}$$

Equation (65) is a key assumption in the later development, but unfortunately it is not readily justified. Physically, we assume that the time scale for the evolution of the single-particle wavefunctions is long compared to the time for the perturbations to develop. Whether the assumption is justified in practice remains to be seen.

The actual perturbation is the two-body interaction minus the mean field, so that the operator V only has matrix elements off-diagonal in both particle states. For our outline of the derivation, we take V to be an external single-particle field. The first-order perturbed wavefunction at time t is

$$\begin{aligned} \left| \psi(t) \right\rangle &= \left| \psi(o) \right\rangle + \frac{1}{i} \int_o^t dt' \sum_{k,k'} e^{-i\Delta\varepsilon t'} V_{kk'} a_{k'}^\dagger a_k \left| \psi(o) \right\rangle \\ &= \left| \psi(o) \right\rangle + \sum_{k,k'} V_{kk'} \frac{\left(e^{-i\Delta\varepsilon t} - 1\right)}{\Delta\varepsilon} a_{k'}^\dagger a_k \left| \psi(o) \right\rangle \qquad (66) \\ \Delta\varepsilon &= e_{k'} - \varepsilon_k \end{aligned}$$

where we have started from the mean-field wavefunction at t=0. We next substitute the perturbed wavefunction in Eq. (4) to get a new dynamic equation. The equation of motion for the diagonal density matrix in the instantaneous basis of H_{MF} depends only on the perturbation,

$$\frac{dn_i}{dt} = \frac{d}{dt}\langle\psi|a_i^\dagger a_i|\psi\rangle = \frac{1}{i}\langle\psi|[a_i^\dagger a_i,\hat{V}]|\psi\rangle$$

$$= \frac{1}{i}\langle\psi|a_i^\dagger[a_{ij}\hat{V}] + [a_i^\dagger,\hat{V}]a_i|\psi\rangle \qquad (67)$$

$$= \frac{1}{i}\sum_j V_{ij}\ [\langle\psi|a_i^\dagger a_j|\psi\rangle - \langle\psi|a_j^\dagger a_i|\psi\rangle]$$

When the perturbed wavefunction (66) is inserted into (67), the righthand side consists of terms of first, second, and third order in V. The first-order terms may be included in the mean field and are not of interest. The third-order terms are neglected in comparison to the second-order terms. These terms required the evaluation of operator expectation values involving four operators. A typical expectation value is

$$\langle\psi(o)|a_i^\dagger a_j\ a_k^\dagger a_{k'}|\psi(o)\rangle = \delta_{k'i}\ n_i\ \delta_{jk}\ (1-n_j) \qquad (68)$$

After some simplification, the result for the dynamic equation is

$$\frac{dn_i}{dt} = \sum_j \frac{2\sin\Delta\epsilon t}{\Delta\epsilon}\ V_{ij}^{\ 2}\ (n_j(1-n_i) - n_i(1-n_j)) \qquad (69)$$

The sine function of $\Delta\epsilon$ is a representation of the delta function, so in the limit where there are enough levels so that $\Delta\epsilon$ takes on values small compared to the inverse time scales of interest, we can express the final result as

$$\frac{dn_i}{dt} \equiv 2\pi\sum_j \delta(\epsilon_i-\epsilon_j)\ V_{ij}^{\ 2}\ (n_j(1-n_i) - n_i(1-n_j)) \qquad (70)$$

This is recognizable as Fermi's golden rule, applied particles rather than to the system as a whole. The only consequence of the many-particle context, besides the mean field, is the presence of occupation factors in the formula.

The correponding formula for a perturbation due to a two-particle interaction is

$$\frac{dn_i}{dt} \cong 2\pi \sum_{\substack{ii'\\jj'}} \langle ii'|V|jj'\rangle^2 \, \delta(\epsilon_i+\epsilon_{i'}-\epsilon_j-\epsilon_{j'}) \, [n_j n_{j'}(1-n_i)(1-n_{i'}) - n_i n_{i'}(1-n_j)(1-n_{j'})] \tag{71}$$

It might also be interesting to consider perturbations of the form of couplings between particles and vibrations. Labelling the vibration by q, the formula describing the effect of the vibrations on the single-particle density is

$$\frac{dn_i}{dt} = 2\pi \sum_{j,q} \langle i|V|jq\rangle^2 \left[\delta(\epsilon_j+\epsilon_q-\epsilon_i)(n_j-n_i)(1+n_q) + \delta(\epsilon_i+\epsilon_q-\epsilon_j)(n_j-n_i)\, n_q\right] \tag{72}$$

To summarize the theory, the mean-field approximation is used as a basis of the representation of the single-particle density matrix. The off-diagonal matrix elements evolve by the mean-field Hamiltonian, while the diagonal matrix elements evolve by Eq. (71). It is easy to see that the theory conserves energy. The only difference from the mean-field theory, the changing of the diagonal density matrix elements, gives an energy change

$$\frac{dE}{dt} = \sum_i \epsilon_i \frac{dn_i}{dt} \tag{73}$$

We substitute Eq. (71) into (73) and see that the sum vanishes, due to the symmetry and energy conservation built into (71). The theory will also conserve momentum if the interaction is translationally invariant.

The theory embodied in Eq. (71) has not yet been calculated to a point that allows a judgement about its adequacy. One attempt at a calculation was made by Wong and Davies,[15] who apply mean-field theory and Eq. (71) to collisions of ^{16}O on ^{16}O and ^{40}Ca on ^{40}Ca. Unfortunately, these authors used as a basis the time-evolved eigenstates of the initial mean-field Hamiltonian, rather than the instantaneous eigenstates of H_{MF}.

In that basis, there are very few levels crossings, and the energy-conserving delta function prevents practically all collisions from occurring. The reason why that happens may be seen in a momentum space representation. The occupied and unoccupied states are concentrated at momenta below and above the Fermi momentum, respectively, with equal probability for positive and negative momenta due to the parity symmetry of the initial state. We have seen that in the mean-field collision dynamics the momenta of the particles do not

change very much. So in the collisional geometry of the Fermi surface with two intersecting spheres, the unoccupied states will remain at a higher energy than the occupied states.

Another approach to introduce collisional dynamics is the theory of Nörenberg, et al.[16] Here the basis of states is the set of instantaneous eigenstates of H_{MF}, as required by (71). However, the initial occupation numbers of these states are not taken from the time-dependent mean-field wavefunction, but are assumed to be 0 or 1, depending on the occupation probability in the initial state. It is also assumed that the level crossings are distinct, occurring one at a time. Then the transitions can be calculated by the Landau-Zener formula [HW],

$$P = \exp\left(-2\pi \frac{V^2}{\dot{\varepsilon}_i+\dot{\varepsilon}_j-\dot{\varepsilon}_k-\dot{\varepsilon}_\ell}\right) \tag{74}$$

In constrast, the perturbation theory limit becomes valid when many level crossings take place over the range of time required for an individual transition. Sketching the energy of a single-particle level as a function of time or of some collective coordinate, the two limits are shown in Fig. 11.

The number of level crossings in a heavy ion collision can be estimated with a Fermi gas model. The state of maximum compression is approximated by the intersecting sphere momentum distribution. In the diabatic picture, the energy of single-particle states change smoothly during the collision process, so that an unoccupied state must cross all unoccupied states having lower energy. In this way, we can examine a particular momentum state in the intersecting Fermi sphere, and compute how many unoccupied states were crossed. If each nucleus starts with a momentum p per particle in the center-of-mass frame, then a particle at the tip of the Fermi surface crosses a number of single-particle states given by

$$N = (2\pi p/P_F)\ \frac{A}{4} + \mathcal{O}(p^2) \tag{75}$$

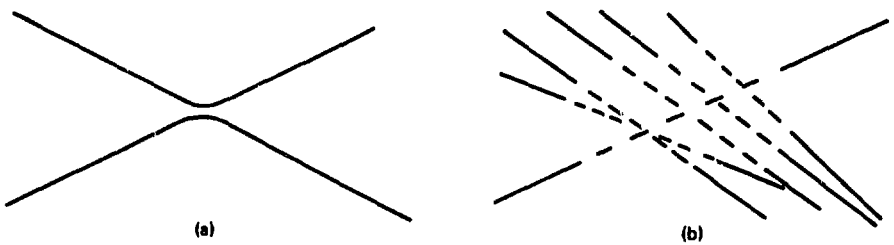

Fig. 11. Sketch of single-particle level crossing for situations in which Landau-Zener formula would be valid, and for which perturbation theory would be valid.

In this equation we count only spatial states of a given kind of nucleon; if both spin orientations are counted, the number should be doubled. The energy change of the particle during the diabatic transformation is

$$\Delta E \sim \frac{\hbar^2}{m} p P_F + \mathcal{O}(p^2) \tag{76}$$

so the energy spacing of the crossings is

$$\Delta E/N \approx \frac{P_F^2}{m} \frac{2}{\pi A} \approx 50/A \text{ MeV} \tag{77}$$

This should be compared with a typical matrix element of the two-particle interaction. The most important matrix elements are of the pairing type, involving particle degenerate energy states. These may be estimated using a zero-range interaction having a strength consistent with the mean-field potential. Calling the strength of the interaction v_o, the volume of the system $\mathcal{V}$, the estimate is

$$\langle i\bar{i} \mid v_o \delta^3(r'r') \mid j\bar{j} \rangle \approx \frac{1}{2} \frac{v_o}{\mathcal{V}} = \frac{1}{2} \frac{v_o \rho_o}{A} \approx \frac{U(\rho_o)}{2A} \approx \frac{25}{A} \text{ MeV} \tag{78}$$

This energy is smaller than the energy spacing in Eq. (76), so the approximation of separated crossings is reasonable at low energies. At higher energies the phase space increases more rapidly, and the perturbation limit is more appropriate.

The Uehling-Uhlenbeck Equation

Equation (71) can be reduced to classical physics in the treatment of large systems with slowly varying potential fields.[17] In that case the eigenstates of H_{MF} are well approximated by wavepackets localized in both momentum and position. The occupation number of the states is then just the phase space occupation probability given by the Wigner function

$$n_i \sim f(p,r) \tag{79}$$

To make the formula completely classical, we also use Born approximation for the particle-particle scattering cross section,

$$\frac{d\sigma}{d\Omega} \approx \frac{2\pi}{v} \int \frac{p_3^2 dp_3}{(2\pi)^3} \langle p_1 p_2 \mid V \mid p_3 p_4 \rangle^2 \, \delta(\epsilon_1 + \epsilon_2 - \epsilon_3 - \epsilon_4) \tag{80}$$

with v the relative velocity of the particles. Then the dynamic equation is

$$\frac{Df(p,r)}{Dt} = \int \frac{dp^3_1\ d^3p_2\ d^3p_3\ d\Omega_3}{(2\pi)^9} \times v \frac{d\sigma}{d\Omega} \left[f(p_1,r)f(p_2,r)\left(1-f(p_3,r)\right)\left(1-f(p,r)\right) - f(p,r)f(p_3,r)\left(1-f(p_1,r)\right)\left(1-f(p_2,r)\right)\right] (2\pi)^3\ \delta^{(3)}\left(p_1+p_2-p_3-p\right) \quad (81)$$

where the total derivative D/Dt represents the entire lefthand side of Eq. (24). This form was first proposed by Uehling and Uhlenbeck.[17] It is the Boltzmann equation with the collision integral modified by the Pauli blocking factors (1-f). This equation is attractive for consideration in the theory of intermediate energy collisions, because it encompasses both the mean-field physics valid at low energies, and the independent collision dynamics applicable at high energies.

The numerical solution of the Uehling-Uhlenbeck equation is difficult, but is undoubtedly within reach of present-day computational techniques. I shall describe one method for solving the equation that has been pursued by the Michigan State University group.[18] The method is based on the Particle-in-Cell technique of numerical hydrodynamics.[19] The system is described by a set of test particles, each having specified momentum and position. The density of these particles in phase space represents the distribution function f(p,r). If the particles obeyed Newtonian mechanics within the mean field, the distribution function would evolve according to the Vlasov equation. The Newtonian equations are integrated with the particle positions calculated at discrete time steps, t+Δt, t+2Δt, etc. The particle positions are updated by the equation

$$\vec{r}_i(\Delta t) = \vec{r}_i(o) + p_i(\Delta t/2)\Delta t/m \quad (82)$$

where p(Δt/2) is the momentum of the particle at the midpoint of the time interval.* To find the momentum vectors at the half time steps, we use the equation

$$\vec{p}_i(\Delta t/2) = \vec{p}_i(-\Delta t/2) + \vec{F}_i(o)\Delta t \quad (83)$$

where $F_i(o)$ is the force at t = 0. The force is calculated by dividing space up into cells. The density in each cell is determined by counting the number of test particles n in that cell,

$$\rho(r) = \frac{n}{N(\Delta x)^3} \quad (84)$$

*The algorithm is an order of Δt more accurate using the momentum at the midpoint rather than at the initial time.

where N is the number of test particles used to represent one physical particle. The potential field of the cell is specified by some function of the density, and the force is determined from the difference in potentials in adjacent cells,

$$F_x(r) = \frac{U(\rho(i,j,k0)-U(\rho(i+1,j,k))}{\Delta x}, \text{ etc.,} \qquad (85)$$

where the point r lies between the midpoints of cells (i,j,k) and (i+1,j,k).

The collision integral in Eq. (81) is calculated by simulating nucleon-nucleon collisions between the test particles. Each test particle is permitted to interact with 1/N of the other test particles in a way that produces the required scattering cross section for isolated nucleons. The Pauli blocking factors are included by accepting or rejecting each collision in a probabalistic way. We examine the final state of each collision, constructing a sphere about the phase space coordinate of each particle. The phase space density f is determined by counting the number of test particles in that sphere. The collision is accepted with a probability $(1-f_p)$ $(1-f_p')$, using a random number generator to make the probabalistic decision.

The numerical parameters that enter the calculation are the cell size, the number of test particles to represent one physical particle, and the time step. We have not yet made a systematic study of the parameter requirements to achieve a definite accuracy, but have only done some exploratory calculations. In Ref. 18 we used cells of 2 fm on a side, which seems adequate for short time intervals, but becomes faulty after times of the order of 100 fm/c: the nuclei do not remain spherical but acquire the square shape of the cells. This situation is rectified by using cells 1 fm on a side, which allows propagation of nuclei to at least 120 fm/c. The number of test particles to represent a physical particle should be large to reduce numerical fluctuations. We found that a nucleus could be described reasonably well with about 10 test particles per occupied cell. Then the numerical fluctuations in the density are of the order of 30%, which seems tolerable in the calculation of the forces. Thus with cells 1 fm on a side, the number of test particles is 50 times the number of nucleons. The requirements on the time step are that the particle travel only a small fraction of cell length and that the collision probability be small during one step. In practice, t=0.5 fm/c seems adequate, and we have used that value. In our present studies, we assume an isotropic cross section of 4 fm^2.

An important test of the numerical scheme is to study the behavior of a nucleus by itself. Besides maintaining its overall shape and density, it should not leak particles, and the momentum distribution should be a sharp-edged Fermi distribution. With the above numerical parameters, we find that less than one nucleon leaks out of an ^{16}O nucleus in a time 120 fm/c, which should be satsifactory to

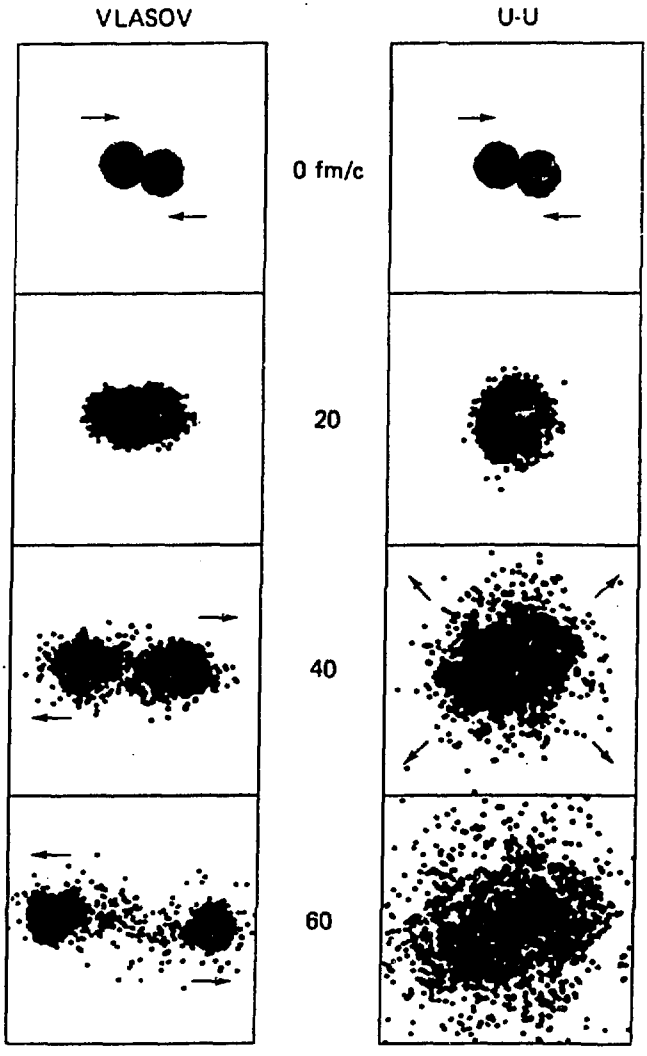

Fig. 12. Collisions of $^{12}C + ^{12}C$ at 84 MeV/n, calculated by J. Aichelin.[21] The lefthand column shows the positions of the test particles, evolved according to the Vlasov equation with the soft potential function, Eq. (52). In the righthand column, the collision integral is included in the evolution equation. The numerical parameters in these calculations are Δt=0.5 fm/c, cell size Δx=1 fm, and N=100 test particles/nucleon.

treat large cross section phenomena for energies down to 25 MeV/n. One check on the effectiveness of the Pauli blocking algorithm is to record the fraction of collisions that are blocked in a nuclear ground state. We find that for ^{16}O, 90% of the collisions between particles are blocked.

We next examine collisions between nuclei. Figure 12 shows the projection of test particles on the x,z plane for collisions of ^{12}C on ^{12}C at 84 MeV/n. The first set of figures shows the theory without collisions, i.e. the Vlasov equation. In that theory, the nuclei go through each other, as they do in TDHF. The prediction of the U-U equation is shown in the second column. The nucleon-nucleon collisions are extremely important, converting the directed motion into a spherically expanding distribution. There is some suggestion[20] that thermal equilibrium may come about very rapidly in collisions at intermediate energy; the study here gives very rough qualitative support to that view.

One observable quantity that can be studied rather easily is the single-particle distribution in the final state. In the laboratory frame, the energy distribution of the emitted particles is quite flat for forward angles, changing to a distribution that falls off steeply with energy at backward angles. This behavior is qualitatively reproduced by the numerical calculations with the Uehling-Uhlenbeck equation.[21] However, it is not completely straightforward to make a quantitative comparison, because the theory provides only a single-particle distribution function, and experiments measure free particles separately from clusters such as alphas which are emitted copiously at the lower energies. Kruse et al. have also studied the single-particle distribution,[22] using a somewhat different technique for particle acceleration in the Uehling-Uhlenbeck equation. They make a clustering correction to the single-particle distribution to obtain the free proton spectrum. They find qualitative agreement between theory and experiment, shown in Fig. 13, with some differences between the theory with and without the mean-field term.

The inclusive single-particle momentum distribution averages over impact parameter and orientation of the collision, losing possible dependences on these parameters. It is possible to regain some of this information with a global analysis of momentum flow. In this technique, the momentum of a large number of particles are measured simultaneously, and the quadrupole tensor of the distribution is determined. One popular definition of this quantity is

$$F_{\mu\nu} = \sum_i \frac{P_\mu(i) P_\nu(i)}{\partial m_i^{-1}}$$

where i labels the different particles emerging from the collision. The tensor tends to be close to isotropic for collisions between

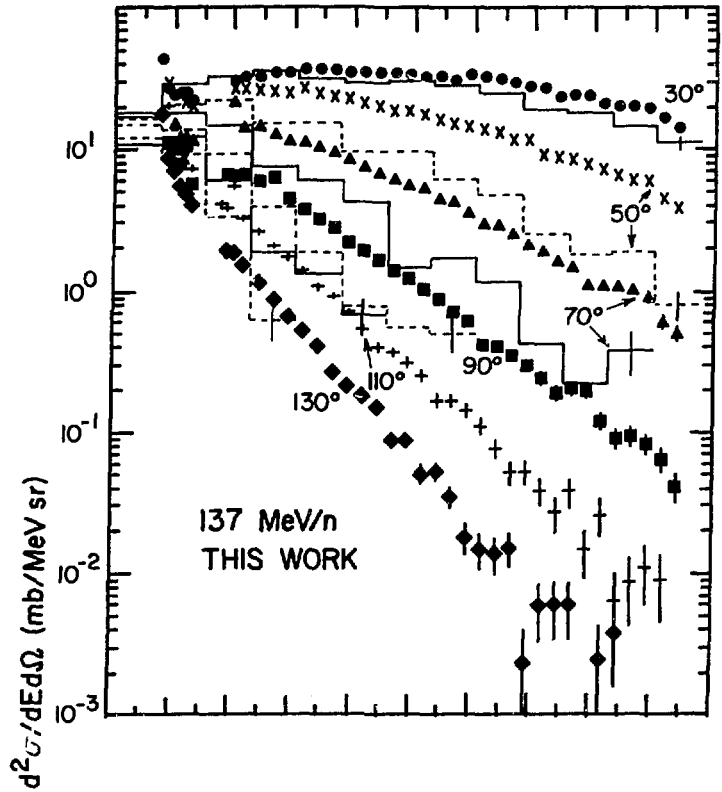

Fig. 13. Proton spectrum from collisions of Ar + Ca at 137 MeV/n. The data[23] are indicated by points, and the theory[22] by histograms.

equal mass target and projectile, but off-diagonal anisotropies are predicted to occur at finite impact parameter in models for which the pressure has other sources besides nucleon-nucleon collisions. Although the anisotropy is rather small, it has a large effect on the orientation of the principal axes of the tensor $F_{\mu\nu}$. The orientation of the longest principal axis, called the flow angle, is thus quite sensitive to the underlying dynamics. Flow angles were recently measured[24] for collisions of ^{40}Ca + ^{40}Ca and ^{93}Nb + ^{93}Nb at energies of 400 MeV/n. In the lighter system, the distribution of flow angles peaked at zero degrees, showing that the anisotropy was small compared to the difference $F_{zz}-F_{xx}$. However, for the heavier system, the most central collisions, defined by the highest multiplicity of secondaries, showed a peaking at a flow angle of 30°. This result is reproduced in the theory based on the Uehling-Uhlenbeck equation. In Fig. 14 is shown the predicted distribution of flow angles for the soft and stiff potential functions.[25] We see that there is some

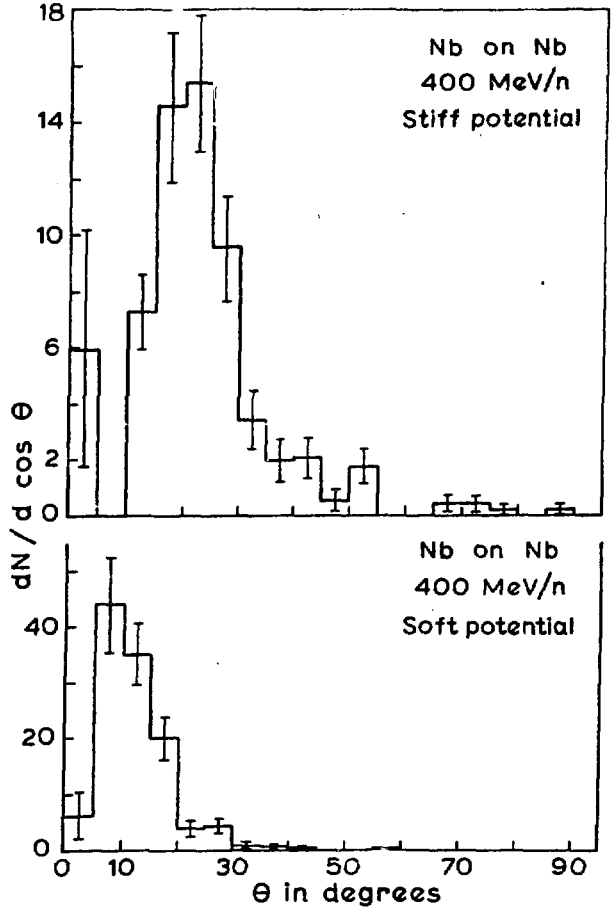

Fig. 14. Predicted flow angles for Nb+Nb collisions at 400 MeV/n, from Ref. 25.

sensitivity to the potential function, with the stiff potential producing more anisotropy. We thus have some hope of extracting the high-density dynamics of heavy-ion collisions from this type of measurement. It is interesting that the sensitivity seems to be greatest at a beam energy of 400 MeV/n; at 200 and 800 MeV/n the flow angle moves to forward direction.[24]

Finally, I would like to conclude with a suggestion that the Uehling-Uhlenbeck equation be applied to the calculation of linear momentum transfer. The data show divisions between regions of nearly complete momentum transfer between target and projectile, and regions where half of the momentum is transferred. At the higher energies where the experiments are done, the mean-field contribution to the longitudinal momentum transfer is small. It will be interesting to see the effect of the nucleon-nucleon collisions in a well-defined theory of the heavy-ion reaction.

References

1. A. Fetter and J. D. Walecka, "Quantum Theory of Many-Particle Systems," McGraw-Hill, New York (1971), p. 149.
2. H. S. Köhler and H. Flocard, Nucl. Phys. A323:189 (1979).
3. H. Tang et al., Phys. Lett. 101B:10 (1981).
4. J. W. Negele, Rev. Mod. Phys. 54:913 (1982).
5. K. T. R. Davies et al., in:"Heavy-Ion Reactions," D. A. Bromley, ed., Plenum, New York (1984).
6. A. Bonasera et al., Phys. Lett. 141B:9 (1984).
7. P. Bonche et al., Phys. Rev. C20:641 (1979).
8. K. T. R. Davies et al., Dynamical Fusion Thresholds, in:"Nuclear Physics with Heavy Ions," P. Braun-Munzinger, ed., Harwood, New York (1984).
9. E. Tomasi et al., Nucl. Phys. A373:341 (1982).
10. J. Barreto et al., Phys. Rev. C27:1335 (1983).
11. J. Randrup, Ann. Phys. (N.Y.) 112:356 (1978).
12. A. Dhar and B. Nilsson, Phys. Lett. 77B:50 (1978).
13. J. R. Nix and A. Sierk, Phys. Rev. C15:2075 (1977).
14. R. Balian and M. Veneroni, Phys. Lett. 136B:301 (1984).
15. C. Y. Wong and K. T. R. Davies, Phys. Rev. C28:240 (1983).
16. W. Nörenberg, Phys. Lett. 104B:107 (1981); H. Yadav and W. Nörenberg, Phys. Lett. 115B:179 (1982).
17. E. Uehling and G. Uhlenbeck, Phys. Rev. 43:552 (1933).
18. G. Bertsch, H. Kruse, and S. Das Gupta, Phys. Rev. C29:673 (1984).
19. F. Harlow and A. Amsden, "Fluid Dynamics," Los Alamos Report LA-4700 (1971).
20. J. Aichelin and G. Bertsch, Phys. Lett. 138B:350 (1974).
21. J. Aichelin and G. Bertsch, to be published.
22. H. Kruse, B. Jacak, H. Stöcker, and G. Westfall, to be published.
23. B. Jacak et al., to be published.

24. H. A. Gustafsson et al., Phys. Rev. Lett. 52:1590 (1984).
25. C. Gale and S. Das Gupta, private communication.